Journal of Solid State Chemistry 181 (2008) 2073–2077

Contents lists available at ScienceDirect

Journal of Solid State Chemistry

journal homepage: www.elsevier.com/locate/jssc

Low-temperature impedance and dielectric relaxation of NiO nanocrystals

Lijuan Chen, Liping Li, Guangshe Li *

State Key Laboratory of Structural Chemistry, Fujian Institute of Research on the Structure of Matter and Graduate School of Chinese Academy of Sciences, Fuzhou 350002, PR China

ARTICLE INFO

Article history:
Received 26 August 2007
Received in revised form
15 January 2008
Accepted 10 April 2008
Available online 3 May 2008

Keywords:
Nio nanocrystals
Low temperature conductivity
Dielectric

ABSTRACT

Low-temperatures impedance and dielectric properties of NiO nanocrystals as a function of particle size were investigated by alternative current impedance spectra. It is found that NiO nanocrystals showed distinct bulk and grain boundary conductions at low temperatures, which were almost the same within the experimental error during the decreasing and the subsequent increasing temperature processes. This result indicated that no further protons are formed during these temperature cycles. The conductivities are also highly dependent on the particle size. As the particle size reduced, the conductivities of NiO nanocrystals increased to show a maximum. Further particle size reduction less than 8.9 nm led to a sudden decrease in conductivity. The corresponding activation energies showed a minimum with varying the particle size. These observations were most likely due to the balance between the concentration of charge carriers, holes and protons.

1. Introduction

Oxide nanocrystals have shown many great potential applications including nanoelectronics, optoelectronic devices [1], humidity sensors [2], gas sensors [3], flat panel displays, field emitters [4], light emitting diode [5], and electrodes in solar cells [6], because of the significant quantum size effects as characterized by distinct electric conductivity and dielectric response from the bulk [7]. It is well known that almost all nanocrystals are strong getters of plenty of adsorption species such as water molecules which may have impacts on the total conductivity at small particle sizes. Therefore, it is very important to precisely determine the conductivities of the nanocrystals by fully taking into account the impacts of hydrated surfaces and particle sizes. In the previous literature work, high-temperature impedance spectroscopy is frequently used to determine the conductivity of the nano-solids, which deserves further investigation because the elevated temperatures might lead to variations in both particle sizes and surface hydration concentration and therefore put big uncertainties in conductivities. For example, Ahmed et al., [8] investigated the temperature dependence of conductivity of In-doped $BaZrO_3$ and found that the removal of the absorbed water produced a decrease in conductivity. Our recent work [9] showed that surface sulfation led to one order of magnitude of conductivity decrease in tetragonal ZrO_2 nanocrystals. Comparatively, low-temperature impedance spectroscopy appears promising in precisely determining the conductivity of nanocrystals since there are no variations in the chemical compositions or particle sizes, and in particular the protonic conductivity from the hydrated surfaces becomes less mobile at low temperatures [10]. Therefore, low temperature impedance spectra are beneficial for in-depth understanding of the electrical properties of nanostructured materials for technological applications.

Dielectric relaxation is another important physical process that is closely relevant to the electrical properties of semiconducting materials [11]. The mechanism of dielectric relaxation could be indicated by the conduction activation energy and relaxation energy. For microcrystalline ceramics or nanocomposite, the polarization relaxation process is highly related to the grain interior or ac conductivity, and the activation energy corresponding to the relaxation process is close to or less than that of ac conductivity [12–16]. However, for nanostructured materials, there exist plenty of defects which vary with the temperature, therefore it is difficult to investigate the dielectric relaxation accurately. Up to date, no sufficient experimental data are available as to the mechanism of dielectric relaxation.

NiO is a typical p-type semiconductor. When the physical dimension of NiO is reduced into nanoscale regime, the conductivity increases by six to eight orders of magnitude as determined by high temperature electrical measurements [17,18], while the influences of hydrated surface and particle size coarsening have been excluded as the causes of the conductivity changes. In this work, we report on the particle size dependence of conductivity and dielectric properties of NiO nanocrystals at low temperatures from room temperature down to 173 K. The activation energies that are responsible for the bulk and grain

* Corresponding author. Fax:+86 591 83714946.
E-mail address: guangshe@fjirsm.ac.cn (G. Li).

0022-4596/$ - see front matter © 2008 Elsevier Inc. All rights reserved.
doi:10.1016/j.jssc.2008.04.012

boundary conduction were indicated. It is found that activation energy for the relaxation process was almost same or less than that for bulk conduction for all sized NiO nanocrystals.

2. Experimental details

Nickel oxide nanocrystals were prepared through a two-step process. In the first step, precursor of $Ni(OH)_2$ was prepared by a chemical precipitation method. Then NiO nanocrystals were obtained to have different particle sizes by annealing the precursor at given temperatures in air for 3 h. Details of sample preparation have already been reported elsewhere [19].

Complex impedance measurements were performed in air on compressed pellets of about 1.2 mm in thickness and 7 mm in diameter. Conducting silver paste was painted on both faces of the pellets and then pre-dried at 373 K for 30 min prior to the impedance measurements. Such a pretreatment allows electrode curing without changing the surface hydration since physisorbed water is reversible at $T<400$ K. The impedance measurements were then carried out in a frequency range from 20 Hz to 1 MHz and at an oscillation voltage of 1.0 V using a precision LCR meter (Agilent 4284A). The measurement temperature was controlled from room temperature down to 173 K at an interval of 10 K. The impedance data were analyzed by an equivalent circuit model using the least-squares refinement program EQUIVCRT [20].

3. Results and discussion

TEM image (Fig. 1) showed that the as-prepared NiO nanocrystals consisted of tiny rounded particles. Fig. 2a shows the complex impedance plots for 8.9 nm NiO that were measured at given temperatures. It is seen that the impedance spectra are temperature dependent. At room temperature, the impedance spectrum is composed of a full semicircular arc at low frequencies and a partial one at high frequencies, which are, respectively, assigned to the grain boundary and bulk conduction [21]. As the temperature was reduced to 273 K, the high frequency semicircular corresponding to the bulk conduction became more apparent. Interestingly, the impedance spectra are also particle size dependent. For NiO nanocrystals with the particle size smaller than 10 nm, two semicircular arcs were observed. With increasing the particle size, as shown in Fig. 2b for 24.3 nm NiO, these two semicircular arcs overlapped. When the particle size was as large as 59.1 nm, only one arc was observed (Fig. 2c). Although NiO nanocrystals have different particle sizes, the temperature dependence of resistance is quite similar, indicating a similar conduction mechanism.

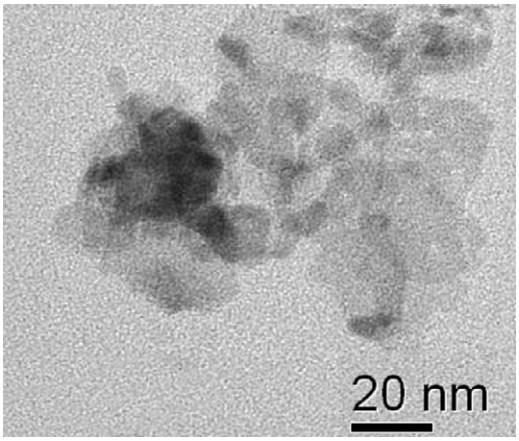

Fig. 1. TEM image of 8.9 nm NiO.

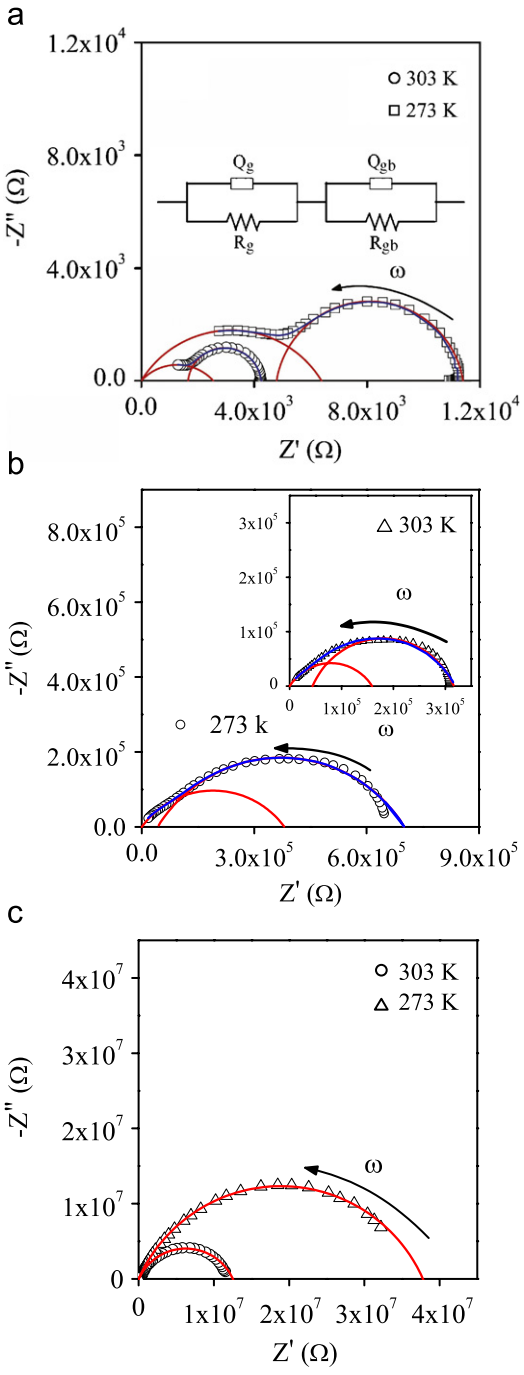

Fig. 2. Complex plane plots for (a) 8.9 nm, (b) 24.3 nm, and (c) 59.1 nm NiO at room temperature and 273 K. Inset of (a) is the equivalent circuit. The raw impedance data (symbols) are fitted using a double resistor-constant phase elements (RQ) series equivalent circuit (solid lines).

Impedance data were fitted to an equivalent circuit model that contains two parallel combinations of resistance, R, and constant phase elements, Q, connected in series (inset of Fig. 2a) with impedance $Z_Q=[A(j\omega)^n]^{-1}$, where A and n are constants for a given set of experimental data, and ω is the angular frequency [21,22]. The fitting results using the equivalent circuit matched well the experiment data as indicated by the solid line in Fig. 2. The bulk and grain boundary conductivities are evaluated from the best fit of the bulk and grain boundary impedance arcs. With

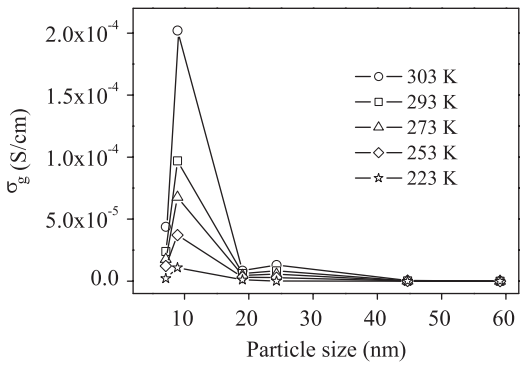

Fig. 3. Particle size dependence of bulk conductivity of NiO nanocrytals at different temperatures.

lowering the temperature, the conductivities decreased. For example, the bulk conductivity for 8.9 nm NiO changed from 2.02×10^{-4} S/cm at room temperature to 3.82×10^{-7} S/cm at 173 K while the grain boundary conductivity decreased from 1.67×10^{-4} S/cm at room temperature to 3.82×10^{-7} at 173 K, respectively. Besides the temperature dependence, both bulk and grain boundary conductivities of NiO nanocrystals are also highly dependent on the particle size. Fig. 3 shows the particle size dependence of bulk conductivity of NiO nanocrystals at given temperatures. It can be seen that bulk conductivities increased greatly to give a maximum with particle size reduction to 8.9 nm at a given temperature. Further reducing the particle size to 7.1 nm led to a sudden decrease in conductivity. To understand the cause of the maximum conductivity (Fig. 3), we have to consider the factors that are responsible for the bulk conductivity. First, the bulk conductivity of NiO nanoparticles might be primarily contributed by the holes and protons because (1) NiO is a p-type semiconductor and (2) NiO nanoparticles may show proton conduction for their highly hydrated surfaces [23] as is for almost all oxide nanoparticles. With regards to the protonic contribution, particle size reduction would give the enlarged surface area and enhanced surface hydration which are expected to produce a promoted conductivity. While, when the dimension of NiO reduced smaller than a certain particle size (e.g., 8.9 nm), the defect concentration might be significantly increased as indicated by the color change from green to dark with particle size reduction. Since these defects including nickel vacancies or interstitial oxygen [24–26] could act as the traps of the holes, the bulk conductivity would be decreased. Therefore, it is most likely that the observation of maximum conductivity (Fig. 3) could be a consequence of the balance between the concentration of charge carriers, holes and protons.

Fig. 4 shows the temperature dependences of the conductivities for the bulk and grain boundary conduction of 7.1 and 8.9 nm NiO during the decreasing and the subsequent increasing temperature process. It can be seen that the conductivities of grains (also grain boundary) for both cycles were nearly the same within the experimental error, which indicated that the conductivity is reliable and that no further protons are formed during this temperature cycle.

Fig. 5 summarizes the temperature dependences of bulk and grain boundary conductivities for all particle sizes of NiO nanocrystals. The slopes were used to calculated the activation energies in terms of the Arrhenius law [27]

$$\sigma = (\sigma_0/T)\exp(-E/k_B T) \quad (1)$$

where E is the activation energy, k_B is the Boltzmann constant, σ_0 is a constant related to the density of charge carriers, and T is the absolute temperature. The activation energies of bulk (E_g) and

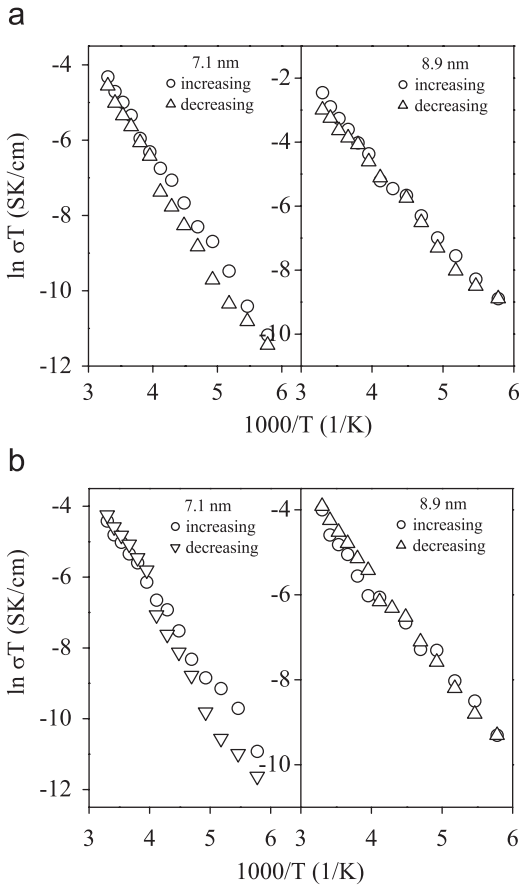

Fig. 4. Temperature dependences of (a) bulk and (b) grain boundary conductivities of 7.1 nm and 8.9 nm NiO during the increasing and the subsequent decreasing temperature processes.

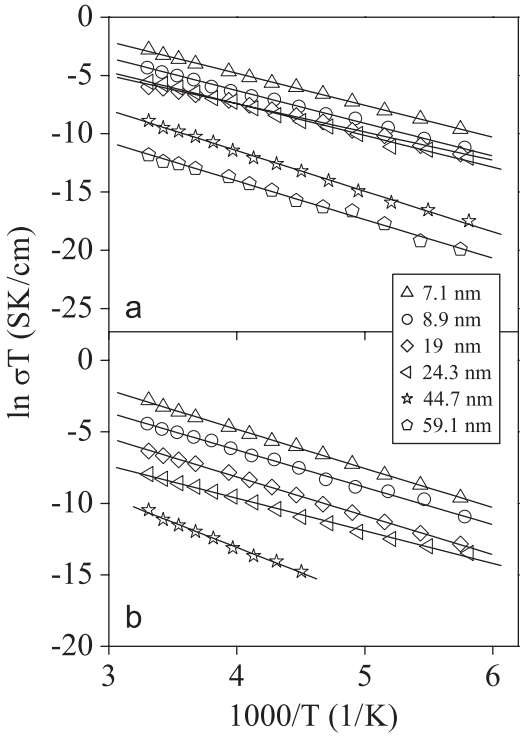

Fig. 5. Temperature dependences of (a) bulk and (b) grain boundary conductivities of NiO nanocrystals at given particle sizes.

Table 1
Activity energies for the bulk (E_g) and grain boundary (E_{gb}) conduction as well as the activation energy (E_τ) for the relaxation processes of NiO nanocrystals at different particle sizes

Particle size (nm)	E_g(eV)	E_{gb}(eV)	E_τ(eV)
7.1	0.242 ± 0.002	0.225 ± 0.006	0.220 ± 0.005
8.9	0.235 ± 0.002	0.226 ± 0.002	0.221 ± 0.003
19	0.208 ± 0.004	0.234 ± 0.002	0.199 ± 0.007
24.3	0.234 ± 0.005	0.196 ± 0.004	0.234 ± 0.006
44.7	0.299 ± 0.005	0.304 ± 0.009	0.3039 ± 0.012
59.1	0.285 ± 0.004	–	–

grain boundary (E_{gb}) conduction are presented in Table 1. It is seen that the values of E_g and E_{gb} were intermediated in a range from 0.2–0.3 eV, which are very close to the value reported previously for NiO nanocrystals at high temperature [24]. Both activation energies (E_g and E_{gb}) showed a minimum with varying the particle size. Just as what is stated above and previously reported by others [25], the primary charge carriers in NiO nanocrystal are the holes that are associated with the Ni^{2+} vacancies or interstitial oxygen. Therefore, the activation energies for bulk and grain boundary conduction are determined by the concentration of holes and their average hopping distances. During the conducting process, charge carriers of holes migrate between the long-range potential wells. For NiO nanocrystals, a large amount of defects appeared [18], which would result in more Ni^{2+} vacancies or interstitial oxygen favorable for long-term hopping of holes and a decrease in activation energy as well. However when the particle size was reduced below a critical size of 30 nm, the lattice expansion would occur [19], which may give rise to a large hopping distance and an enhanced energy barrier for charge carriers hopping. Therefore, the activation energies for bulk and grain boundary conduction could show a similar increasing trend at smaller particle sizes, which is apparently different from a random fluctuation in activation energy reported in literature [24].

The dielectric properties are strongly influenced by the presence of surface absorbents, grain boundaries, grain size and orientation, the concentration of charge carriers [11]. Therefore, study of the dielectric properties at low temperatures may help to better understand the intrinsic electrical properties of NiO nanocrystals without the disturbance of the variations in the external parameters like surface absorbents or grain boundaries. The dielectric properties of NiO nanocrystals are determined in terms of the permittivity formalism, $\varepsilon^* = 1/iwC_0Z^*(w)$ [22], where $\omega = 2\pi f$ is the angular frequency and C_0 is the vacuum capacitance of the sample holder. Fig. 6a shows the representative frequency dependence of the real part, ε', of relative dielectric constant of 8.9 nm NiO. It is interesting that the variation of ε' with temperature just followed what is described above for bulk conductivity. The ε' value is large at low frequencies irrespective of the measurement temperature, which is likely due to the charge accumulation at the interfaces since the conducting species including holes or protons are unable to exchange with silver electrodes. With increasing the frequency, ε' decreased, which is likely due to the high periodic reversal of the field at the interfaces. Consequently, the contribution of charge carriers to the dielectric constant was reduced [28]. Fig. 6b shows the imaginary part of the relative dielectric constant, ε'', of 8.9 nm NiO. ε'' is characteristic of the dielectric loss. The dielectric loss was almost linear to the frequency, which clearly indicates a large electronic contribution [29].

It is well known that the relaxation time is an important physical parameter that characterizes the dielectric properties.

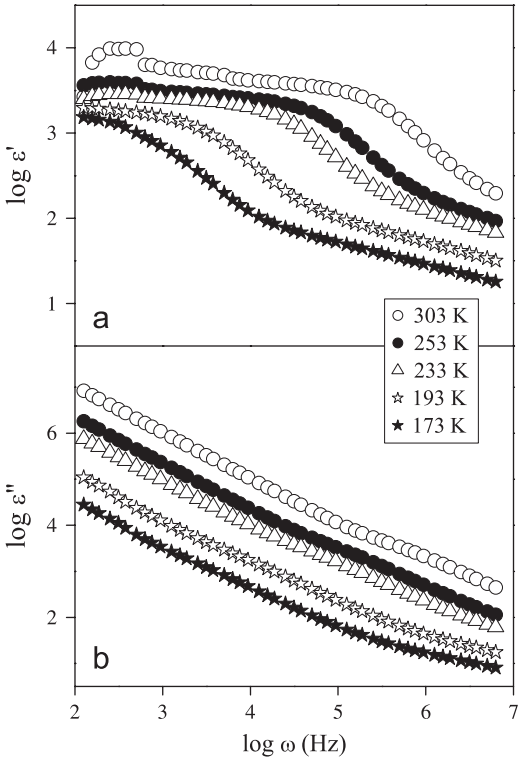

Fig. 6. Frequency dependence of the (a) real part and (b) imaginary part of relative dielectric constant for 8.9 nm NiO at different temperatures.

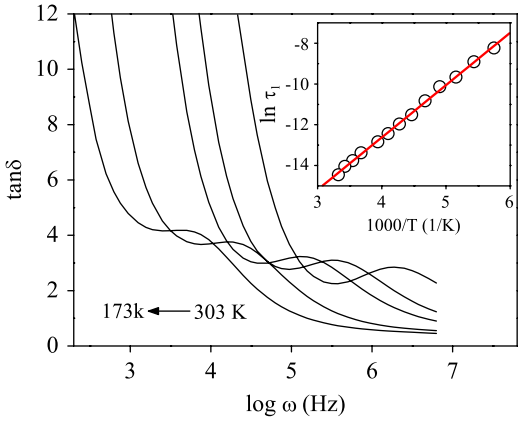

Fig. 7. Loss tangent $\tan\delta$ as a function of frequency for 8.9 nm NiO at different temperatures. Inset shows the Arrehenius plot of $\ln\tau_1$ against $1/T$ for 8.9 nm NiO. Solid lines represent the data fit results using Eq. (4).

Due to the absence of any well-defined loss peak, it seems not possible to calculate the relaxation time directly from ε''. We obtained the relaxation time from the loss tangent. The variation of the loss tangent, $\tan\delta = \varepsilon''/\varepsilon'$, as a function of $\log\omega$ for 8.9 nm NiO is shown in Fig. 7. The signals corresponding to the dielectric relaxation processes are clear. Generally, the dielectric relaxation is expressed by a Debye relaxation relation [30],

$$\varepsilon^* - \varepsilon_\infty = \frac{\varepsilon_s - \varepsilon_\infty}{1+(\omega\tau)^2} - j\frac{\omega\tau(\varepsilon_s - \varepsilon_\infty)}{1+(\omega\tau)^2} \quad (2)$$

where ε_s is the static field dielectric constant, ε_∞ is the high frequency dielectric constant of the material, ω is the applied angular frequency, and τ is the relaxation time which can be

obtained from the frequency at the peaks of ε''. Then, we get

$$\tan\ \delta = \frac{(\varepsilon_s - \varepsilon_\infty)}{\varepsilon_s + \varepsilon_\infty(\omega\tau)^2} = 2\ \tan\ \delta_m \frac{\omega\tau_1}{1+(\omega\tau_1)^2} \quad (3)$$

where $\tan\delta_m$ is the maximum loss at the peak which is nearly the same as a function of temperature as shown in Fig. 7, and τ_1 is equal to $\tau\sqrt{\varepsilon_\infty/\varepsilon_s}$. From Eq. (3), it is obvious that $\tan\delta$ has a maximum at $w\tau_1 = 1.0$. According to the reference [30], $\varepsilon_\infty/\varepsilon_s$ should be temperature independent. Therefore, the dielectric relaxation time τ_1 can follow the same equation as relaxation time τ [10],

$$\tau_1^{-1} = \tau_0^{-1}\ \exp(-E_\tau/k_B T) \quad (4)$$

Here, E_τ denotes the activation energy as required for the dielectric processes, and τ_0 represents the pre-exponential factor and $k_B T$ is the thermal energy.

Inset of Fig. 7 shows the Arrehenius plot of $\ln\tau_1$ against $1/T$ for 8.9 nm NiO. According to the Eq. (4), the slope obtained from the best fit of the experimental data (inset of Fig. 7) is the activation energy E_τ. All calculated E_τ data are listed in Table 1. Comparing with the values of E_τ to E_g and E_{gb} for the same particle sizes, it is found that the activation energy, E_τ, required for relaxation is equal to or less than E_g for all sized NiO. These results indicate that the thermal activation of relaxation process has a close relation to the bulk conduction. On the other hand, the values of E_τ are near the same or less than those of E_g, which implies that the relaxation mechanism is governed by the hopping of holes rather than the dipole-type mechanism, since for the latter case, E_τ is always quite larger than E_g [31].

4. Conclusions

This work reported on the impedance spectra and dielectric relaxation of NiO nanocrystals of different particle sizes at low temperatures. With particle size reduction, the bulk and grain boundary conductivities increased to show a maximum, while the corresponding activation energies varied with the particle sizes to show a minimum. Further, the activation energy for the dielectric relaxation process is almost the same as or less than that for the bulk conduction. These observations were explained in terms of the balance of the carriers of holes and protons as a function of particle sizes.

Acknowledgments

This work was financially supported by NSFC under the contract (No. 20671092, 20773132 and 20771101), National Basic Research Program of China (No. 2007CB613301), a grant from Directional Program of CAS (No. KJCXZ-YW-M05), and in part by Research Foundation of FJIRSM (No. SZD08002-3).

References

[1] Y.K. Che, A. Datar, X.M. Yang, T. Naddo, J.C. Zhao, L. Zang, J. Am. Chem. Soc. 129 (2007) 6354–6355.
[2] M.M. Ahmad, S.A. Makhlouf, K.M.S. Khalil, J. Appl. Phys. 100 (2006) 094323.
[3] L. Schmidt-Mende, J.L. MacManus-Driscoll, Mater. Today 10 (2007) 40–48.
[4] Q. Wan, E.N. Dattoli, W. Lu, Appl. Phys. Lett. 90 (2007) 222107.
[5] S. Shrestha, C.M.Y. Yeung, C. Nunnerley, S.C. Tsang, Sens. Actuators A 136 (2007) 191–198.
[6] A. Subramania, T. Saradha, S. Muzhumathi, J. Power Sources 167 (2007) 319–324.
[7] S. Hara, M. Miyayama, Solid State Ionics 168 (2004) 111–116.
[8] I. Ahmed, S.G. Eriksson, E. Ahlberg, C.S. Knee, M. Karlsson, A. Matic, D. Engberg, L. Börjesson, Solid State Ionics 177 (2006) 2357–2362.
[9] H. Wang, X.Q. Qiu, L.P. Li, G.S. Li, Chem. Lett. 36 (2007) 1132–1133.
[10] S. De, A. Dey, S.K. De, J. Chem. Phys. 125 (2006) 224704.
[11] N.H. Vasoya, V.K. Lakhani, P.U. Sharma, K.B. Modi, R. Kumar, H.H. Joshi, J. Phys.: Condens. Matter 18 (2006) 8063–8092.
[12] Y.H. Lin, M. Li, C.W. Nan, J.F. Li, J.B. Wu, J.L. He, Appl. Phys. Lett. 89 (2006) 032907.
[13] J.B. Wu, C.W. Nan, Y.H. Lin, Y. Deng, Phys. Rev. Lett. 18 (2002) 217601.
[14] A. Dey, A. De, S.K. De, J. Phys.: Condens. Matter 17 (2005) 5895–5910.
[15] N. Ponpandian, P. Balaya, A. Narayanasamy, J. Phys.: Condens. Matter 14 (2002) 3221–3237.
[16] A. Dey, S. De, A. De, S.K. De, J. Nanosci. Nanotechnol. 6 (2006) 1427–1436.
[17] V. Biju, M.A. Khadar, J. Mater. Sci. 38 (2003) 4055–4063.
[18] V. Biju, M.A. Khadar, Mater. Sci. Eng. A A 304–306 (2001) 814–817.
[19] L.P. Li, L.J. Chen, R.M. Qihe, G.S. Li, Appl. Phys. Lett. 89 (2006) 134102.
[20] B. Boukamp, Equivalent circuit (EQUIVCRT. PAS), University of Twente, Twente, 1988-89.
[21] S.M. Haile, D.L. West, J. Campbell, J. Mater. Res. 13 (1998) 1576–1595.
[22] E. Barsoukov, J.R. Macdonald, Impedance Spectroscopy, Wiley, New Jersey, 2005, p. 18.
[23] L.J. Chen, L.P. Li, G.S. Li, Solid State Ionics, in revision.
[24] V. Biju, M.A. Khadar, J. Mater. Sci. 36 (2001) 5779–5787.
[25] S. Nandy, B. Saha, M.K. Mitra, K.K. Chattopadhyay, J. Mater. Sci. 42 (2007) 5766–5772.
[26] E. Antolini, J. Mater. Sci. 27 (1992) 3335–3340.
[27] P. Lunkenheimer, T. GÖtzfried, R. Fichtl, S. Weber, T. Rudolf, A. Loidl, A. Reller, S.G. Ebbinghaus, J. Solid State Chem. 179 (2006) 3965–3973.
[28] P.S. Anantha, K. Hariharan, Mater. Sci. Eng. B 121 (2005) 12–19.
[29] N. Chabchoub, J. Darriet, H. Khemakhem, J. Solid State Chem. 179 (2006) 2164–2173.
[30] M.M. El-Desoky, S.M. Salem, I. Kashif, J. Mater. Sci.-Mater. Electron. 10 (1999) 279–283.
[31] S.J. Lee, K.Y. Kang, S.K. Han, Appl. Phys. Lett. 75 (1999) 1784–1786.